entropy

MDPI

Type of the Paper (Article, Review, Communication, etc.)

Dynamic Mode Decomposition: Group-Level Analysis of the FBIRN Dataset

Firstname Lastname [1], Firstname Lastname [2] and Firstname Lastname [2,*]

[1] Affiliation 1; e-mail@e-mail.com
[2] Affiliation 2; e-mail@e-mail.com
* Correspondence: e-mail@e-mail.com; Tel.: (optional; include country code; if there are multiple corresponding authors, add author initials)

Abstract:

Keywords:

1. Introduction

2. Materials and Methods

2.1. Data Collection

2.2. Estimation of the Spatial Functional Networks

2.3. Estimation of the Functional Network Connectivity

2.4. Estimation of the Dynamic Mode Decomposition

2.4.1. Standard (SVD) DMD

2.4.2. Exact DMD

2.4.3. Comparison of standard vs. exact DMD modes

2.5. Group-Level Decomposition

2.5.1. Demeaning the Data

To allow comparability between subjects, the mean FNC matrix of each subject is removed from the overall subject time course. Note that this is not the mean of each FNC matrix, but the mean FNC matrix—that is, the static FNC matrix—of each subject. Fortunately, MATLAB's minus function allows the subtraction of a vector from all columns of a matrix simultaneously, thus obviating the need for a memory- and time-intensive loop.

2.5.2. Phase Discontinuities

Citation: To be added by editorial staff during production.

Academic Editor: Firstname Lastname

Received: date
Revised: date
Accepted: date
Published: date

When concatenating two or more periodic or semi-periodic time series, one must account for the existence of noncontinuities at sample boundaries. Simply put, while each individual sample time series may be continuous, it is highly unlikely that all members of the ensemble are in phase. As such, some means of either accounting for or avoiding these boundary discontinuities must be employed. Fortunately, there is a simple means to achieve this. Recall that dynamic mode decomposition can be framed as a linear map $\boldsymbol{A}$ between a set of samples $\boldsymbol{X}$ and a related sample set $\boldsymbol{Y}$ such that $\boldsymbol{Y} = \boldsymbol{AX}$ [1]. Importantly, this relation in no way implies that the input data vectors must be sequential. So long as $\boldsymbol{Y}(j) = \boldsymbol{AX}(j)$, there is no need to impose the constraint that $\boldsymbol{Y}(j) = \boldsymbol{X}(j+1)$. Thus, the discontinuity problem may be solved by simply omitting the $(\boldsymbol{X}:\boldsymbol{Y})$ pair which contains the discontinuity. To achieve this, each subjects' data $\boldsymbol{D_s}$ are split into two related sets $\boldsymbol{X}_s$ and $\boldsymbol{Y}_s$ such that $\boldsymbol{X}_s = \boldsymbol{D}_s(1{:}T-1)$ and $\boldsymbol{Y}_s = \boldsymbol{D}_s(2{:}T)$. Group-level sets $\boldsymbol{X}$ and $\boldsymbol{Y}$ are then assembled by concatenating the subject-level sets: $\boldsymbol{X} = [\boldsymbol{X}_1, \boldsymbol{X}_2, \boldsymbol{X}_3, \ldots \boldsymbol{X}_n]$, $\boldsymbol{Y} = [\boldsymbol{Y}_1, \boldsymbol{Y}_2, \boldsymbol{Y}_3, \ldots \boldsymbol{Y}_n]$.

2.5.3. Group-Level Decomposition

Once the group-level set is assembled in this way, group-level dynamic mode decomposition (DMD) proceeds in essentially the same fashion as subject-level DMD.

2.5.4. Group-Level Reconstruction

Removal of the static FNC raises some questions in evaluating DMD reconstruction. For instance, it is no longer meaningful to visually compare the reconstructions' time averages to static FNC.

How to reconstruct a demeaned FNC array?

2.5.5. Time-Resolved Mean Squared Error

Calculation of the time-resolved mean squared error (MSQE) began by reconstructing a single subject time series from the group-level DMD modes and eigenvalues. Two reconstructions were estimated, the first using the complete mode spectrum from each group, and the second using only the six most powerful modes of each group. The mean squared error (MSQE) is estimated between each group reconstruction and a group average dFNC. The usefulness of the subject-demeaned group average dFNC is questionable, as its signal is necessarily near zero at all time points. It may be more informative to compare the reconstruction to a concatenation of subject dFNCs, or a randomly selected subject.

2.5.6. Time-Resolved Amplitudes of Modes

To evaluate the time-resolved trends in the data, the time-resolved values of a set of six connections from the dFNC were plotted as a function of time (Figure []). Single-mode group timecourses are then reconstructed for each of the six modes with the highest power of each group. The predicted time evolution of each mode is then plotted over time (ten standard scans, or 1370 samples) to determine how DMD predicts these modes' evolution.

3. Results

3.1. Group-Level Decomposition

3.1.1. Reconstruction of static FNC

Figure [] depicts the sFNC of each group, as well as that reconstructed from both standard and exact DMD. The most extensive functional connectivity bloc covers the auditory, sensorimotor, and visual systems virtually completely, and weakly anticorrelates with most cognitive control, default-mode, cerebellar, and subcortical regions. This bloc is notably fragmented in schizophrenia patients, in which the correlations between the auditory-sensorimotor and visual systems almost entirely disintegrate. Anticorrelations with cerebellar and subcortical networks also appear weaker in patients than in controls. Statistical testing will be necessary to confirm these differences.

Neither standard nor exact DMD adequately capture the large auditory-sensorimotor-visual functional block. Indeed, even intra-domain correlations—visual-to-visual, sensorimotor-to-sensorimotor—are substantially underestimated in DMD-based reconstructions, leading to fragmented intra-domain modules. Inter-domain correlations are still more poorly captured, with many of the weaker connections lost entirely. Visual networks are reconstructed as anticorrelated with auditory and some sensorimotor networks, a feature entirely at odds with the true sFNC. In general, exact DMD seems to capture a slightly higher proportion of connectivity within the sensorimotor domain than standard DMD, a pattern reversed the visual and inter-domain correlations. Both reconstructions substantially reduce anticorrelations between cerebellar, auditory, and sensorimotor networks.

The cognitive control networks mostly correlate with one another, albeit weakly. Several networks also consistently but weakly correlate with cerebellar and subcortical regions. This cognitive control-cerebellar connectivity is notably more consistent in controls. Both sample groups show fragmentary connectivity between cognitive control and default-mode networks. Controls also show some connectivity between cerebellar, default-mode, and cognitive control regions, a feature mostly absent in patients. Cerebellar regions display strong intra-domain connectivity in both groups. Reconstructions tend to overestimate cognitive control intra-domain connection strength, although this does not form an obvious pattern. Reconstructions also amplify cognitive control-cerebellar and default-mode-cerebellar anticorrelations, to the point of reversing the polarity of several connections.

It is not immediately clear why reconstructed static FNC conforms poorly to ground truth.

sFNC Retained

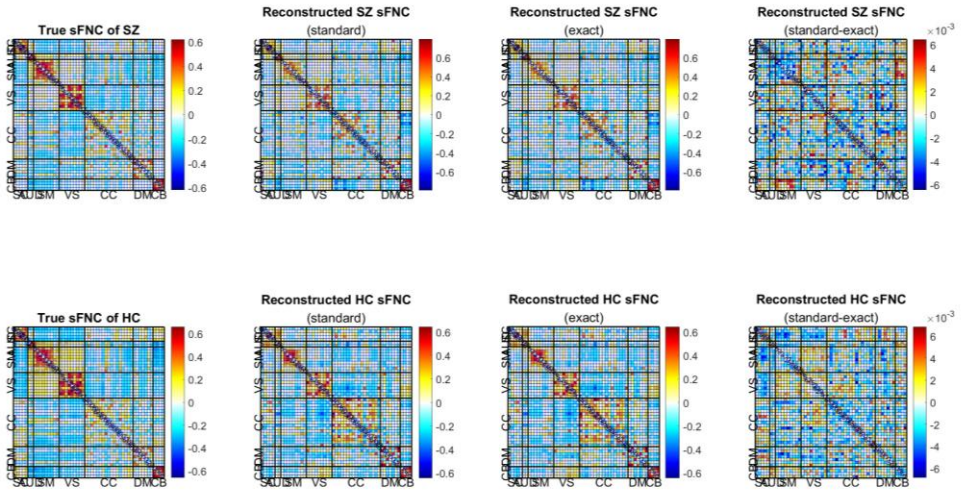

sFNC Removed

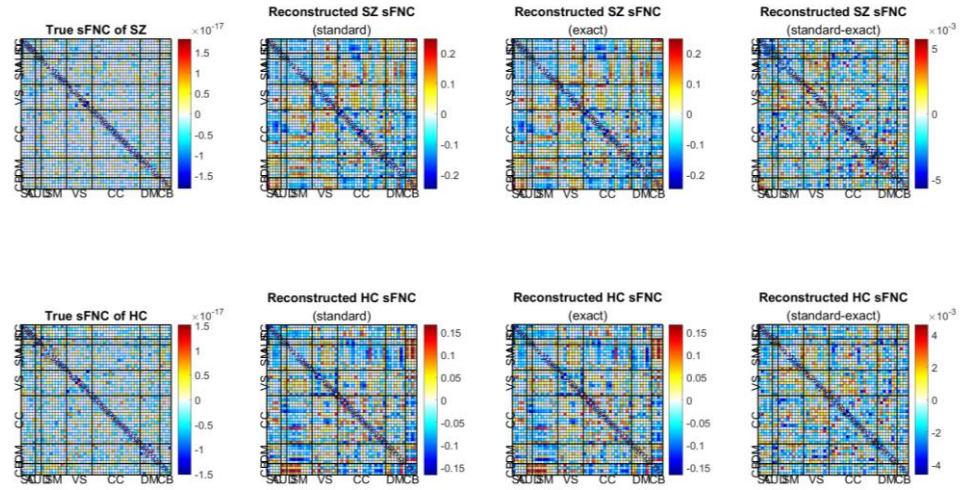

3.1.2. Reconstruction of dynamic FNC

The mean squared error (MSQE) calculated as a function of time reveals some unexpected behavior. A full time-resolved reconstruction of the dFNC using standard DMD starts with an initial MSQE of 0.185879 ($MSQE(1) = 0.185879$) in healthy controls.

Aside from a rise between time points 41 and 60 ($MSQE(41) = 0.168889$, $MSQE(60) = 0.182498$), this error consistently falls over time, although the rate of decline shows a semiperiodic variation. Full dFNC reconstruction using exact DMD modes shows an essentially identical evolution. This general pattern holds in schizophrenia patients, albeit with slightly different starting and ending values ($MSQE(1) = 0.198352$, $MSQE(137) = 0.0965442$) and absent the short rise in the center of the reconstruction. Exact DMD produces statistically identical results.

A partial reconstruction of the dFNC display very different results. When using only the six modes with the highest power, standard DMD of healthy controls starts with a lower MSQE than full reconstruction ($MSQE_{par}(1) = 0.157229$). However, whereas the full reconstruction's MSQE declines with time, the partial reconstruction's MSQE increases to a maximum value of 0.174839 and a final value of 0.168737. Like the full reconstruction, partial reconstruction's MSQE displays semiperiodic variation in its rate of change over time; however, the direction of change is almost universally the opposite of that of the full reconstruction. Partial reconstruction of schizophrenia patients also shows increasing MSQE over time, but MSQE is lower in terms of both absolute value and rate of change ($MSQE_{par}(1) = 0.135638$, $MSQE(97) = 0.14565$, $MSQE(137) = 0.14402$). Exact DMD produces statistically identical results.

These results deserve further examination, as they seem incompatible with the static FNCs generated from these dynamic reconstructions. Full reconstructions of schizophrenia patients appear to overestimate the sFNC magnitude of many connections by over 10%, while an sFNC generated from a six-mode partial reconstruction shows a dynamic range scarcely 10% that of the true sFNC. Similarly, the sFNC based on a partial reconstruction of healthy controls shows a dynamic range of less than 20% of the true sFNC, although the full reconstruction mostly complies with ground truth. Given these enormous disparities in dynamic range, it seems highly implausible that MSQE values of full and partial reconstructions should be comparable. Further investigation into this disparity is clearly necessary.

Removal of the group sFNC from the dynamic FNC makes the problem of calculating the mean squared error still more difficult, as the average subject dFNC becomes uniformly near zero. In such a scenario, MSQE is primarily determined by the magnitude of the reconstruction rather than variation in the signal. The method of using an average dFNC as "ground truth" is likely flawed and should be replaced. Until a suitable replacement method is found, time-resolved MSQE values cannot be treated as meaningful measures of reconstruction accuracy. Another method of establishing reconstruction accuracy must be developed.

sFNC Retained

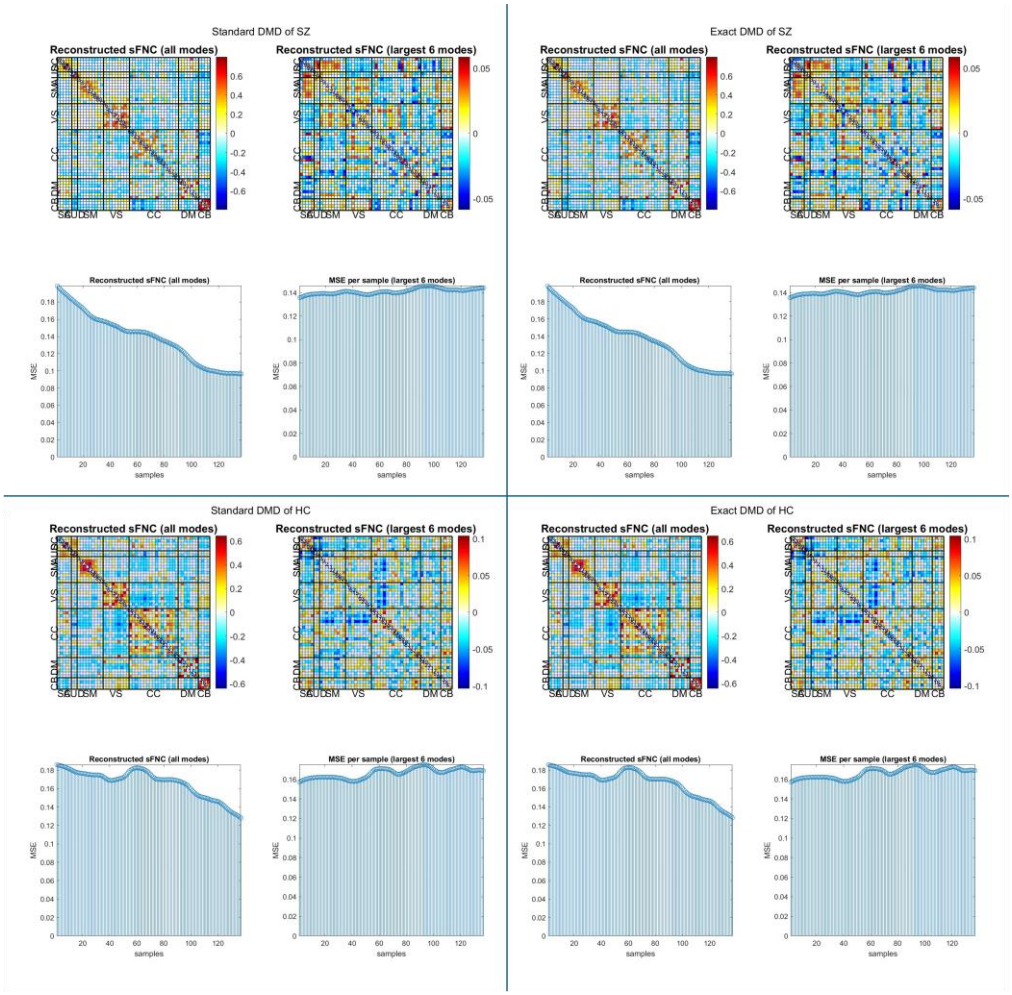

sFNC Removed

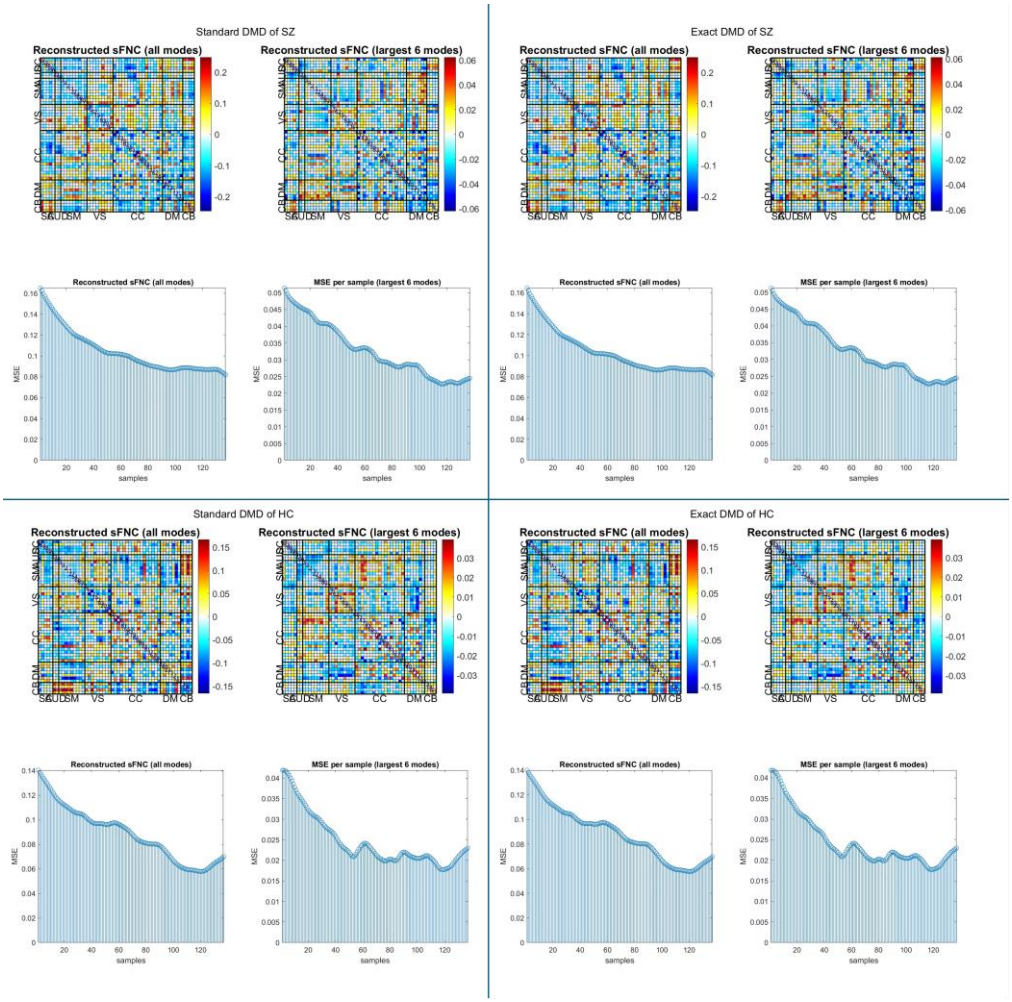

169
170

3.1.3. Group-Level Spectra

171

Removal of scalar subject FNC means produces, at first glance, broadly similar power spectra in controls and patients. The static mode ($f = 0$ Hz) has far and away the largest magnitude in both groups ($HC(0) = 671.84, SZ(0) = 653.07$), with all other frequencies having magnitudes of 210 or less. Controls display two static modes ($f = 0$ Hz), with the smaller having a magnitude of 123.5. Six patient oscillatory modes have magnitudes above 190 ($HC(6.421 \times 10^{-5}) = 208.134$, $HC(69.3932 \times 10^{-5}) = 197.705$, $HC(3.09135 \times 10^{-4}) = 210.735$, $HC(3.4549 \times 10^{-4}) = 192.651$, $HC(1.0908 \times 10^{-3}) = 195.58$, $HC(1.20327 \times 10^{-3}) = 191.143$); all others have magnitudes of 167 or less. The result is a spectrum which appears rather flat save for the mode at $f = 0$ Hz. Omitting this mode from analysis may allow better insight, as it dominates the spectrum at present.

172
173
174
175
176
177
178
179
180
181

A similar pattern plays out in schizophrenia patients, with two notable differences. First, decomposition of the schizophrenia dataset finds not two, but eight static modes ($f = 0$ Hz). Of these, only three exceed a magnitude of 190. Only five modes of the schizophrenia dataset exceed a magnitude of 150, and of these, only one has a nonzero frequency ($SZ(2.9472 \times 10^{-4}) = 168.963$). Overall, schizophrenia modes have noticeably lower magnitudes than their healthy counterparts, and over twice as much power as a percentage of the total is in static frequencies. Schizophrenia patients appear to concentrate a greater proportion of power in low frequencies as a result, but this effect is minor and requires statistical testing.

sFNC Retained

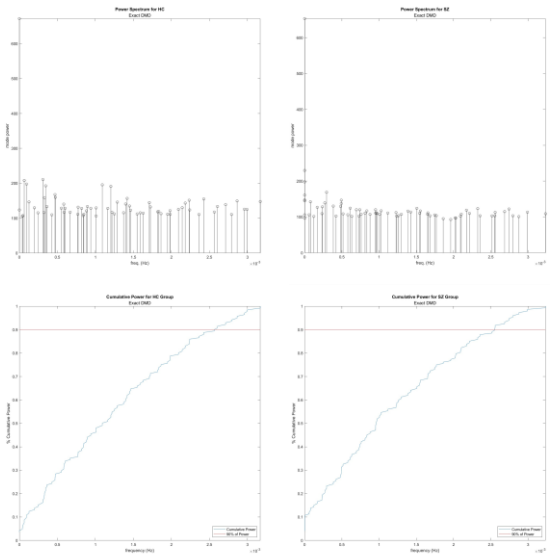

Unsurprisingly, removal of subject mean FNC matrices drastically attenuates the static modes of both patient and control power spectra. Although both patients and controls retain static modes—four and two, respectively—their power is dramatically reduced. Patient static modes now have power of less than 100, and no control static mode exceeds 120. Patient mode power remains generally lower than those of controls, with only six patient modes having power above 100. This may be attributable to the slightly lower number of patients than controls in the dataset, but the author doubts it. Patients possess less than 6% fewer datapoints than controls, while the difference between power spectra magnitudes approaches 20%. The author thus hypothesizes that patients display statistically significant reductions in mode power. Despite this, the relatively flat shape of both spectra result in visually similar cumulative power curves.

Following the initially high powers near zero frequency, the patient power spectrum displays a semiperiodic structure with a period of approximately 1.5×10^{-3} Hz. A cluster of high power occurs between 2×10^{-3} and 2.5×10^{-3} Hz, and another between 3.5×10^{-3} and 4×10^{-3} Hz. A similar pattern is not visually identifiable in the spectrum of healthy controls.

sFNC Removed

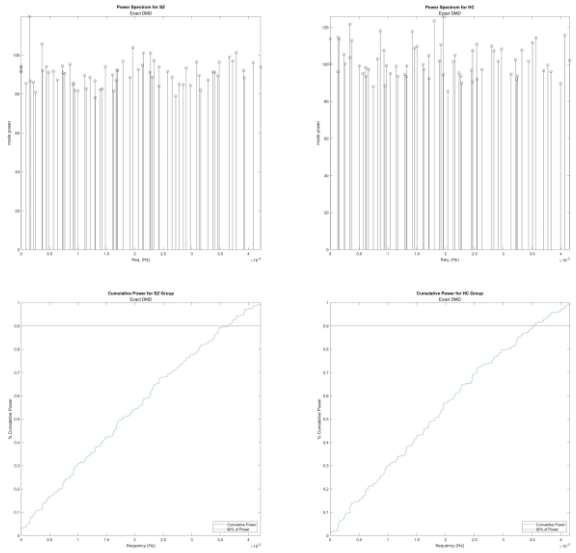

3.1.4. Group-Level Eigenvalue Spectra

Both control and patient eigenvalue spectra cluster around the (1,0) value of the unit circle, suggesting phases near zero and magnitudes near unity. Controls display a single eigenvalue of magnitude $1.0028 > 1$, suggesting a weak increase in oscilliatory amplitude over time. All other control eigenvalues, as well as all schizophrenia eigenvalues, display magnitudes less than, but very close to, unity. In fact, eigenvalue magnitudes are so near unity that one may question whether the increase or decrease in oscillatory amplitude would be noticeable over the course of a typical scan. Additional research on the basics of dynamic systems theory may be necessary to determine the theoretical solution to this question.

sFNC Retained

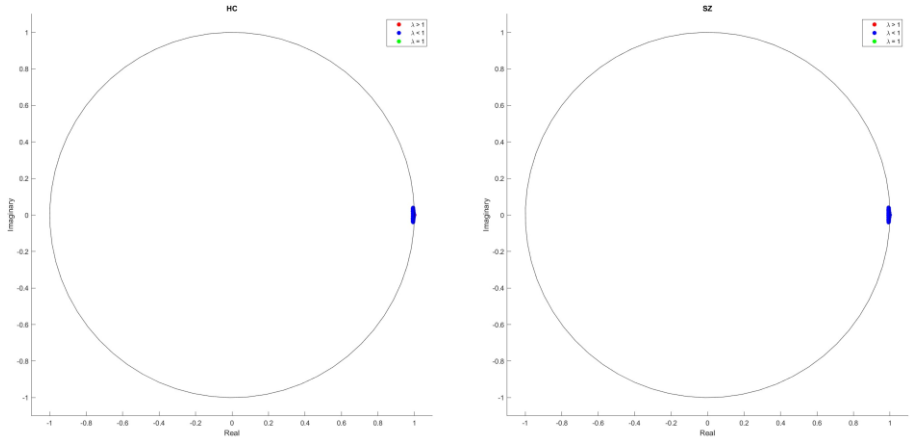

Removal of subject sFNC from each subject time course has minimal effect on the previously described eigenvalue spectra. The most obvious change is that, following the removal of subject sFNC, all group eigenvalues have magnitudes less than unity. They remain, however, tightly clustered near (1,0) value on the unit circle, so much so that it is questionable whether the predicted decay in mode amplitudes would be noticeable over the course of a typical scan.

sFNC Removed

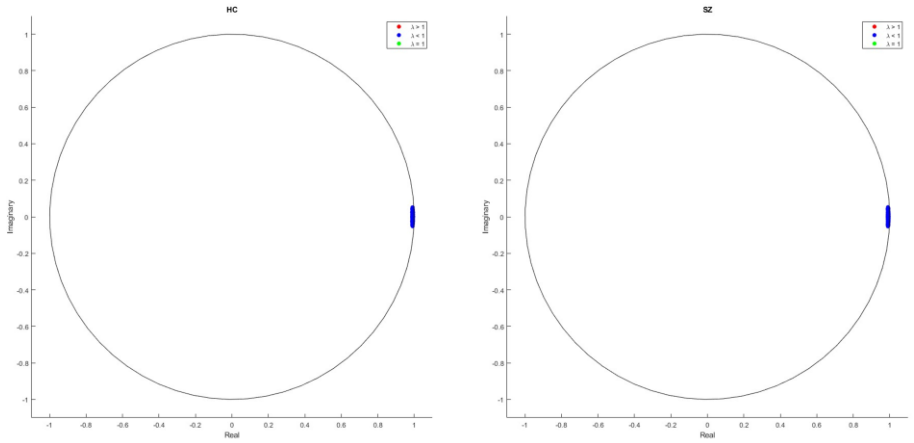

3.1.5. Group-Level Mode Amplitudes Over Time

To evaluate the time-resolved trends in the data, the time-resolved values of a set of six connections from the dFNC were plotted as a function of time (Figure []). Single-mode group timecourses are then reconstructed for each of the six modes with the highest

power of each group. The predicted time evolution of each mode is then plotted over time (ten standard scans, or 1370 samples) to determine how DMD predicts these modes' evolution. For controls, two of these modes have frequencies of zero (static), while the other four are very low frequency. All of the plotted patient modes are static (frequency zero), as a high proportion of patient power is maintained in these modes.

Examination of the figures again shows no meaningful differences between exact and standard DMD, although statistical tests should be employed to confirm this. All selected modes' real amplitudes decay exponentially to zero over time, although the starting amplitude and rate of decay varies between modes. All selected control modes save one decay to near zero after a reconstruction of five standard scans (785 samples). The final mode decays more slowly, but still approaches zero by the end of reconstruction. A similar pattern appears in patients, with all modes decaying towards zero real amplitude. However, the rate of decay is noticeably slower in three of these modes, with two maintaining sizable real amplitudes even by the end of reconstruction (1370 time points). Patients may, then, have more persistent connectivity patterns than controls, in line with previous research suggesting reduced entropy in patients.

As patients and controls possess different modes with different oscillatory frequencies, it is not immediately clear how their trajectories might be compared.

sFNC Retained

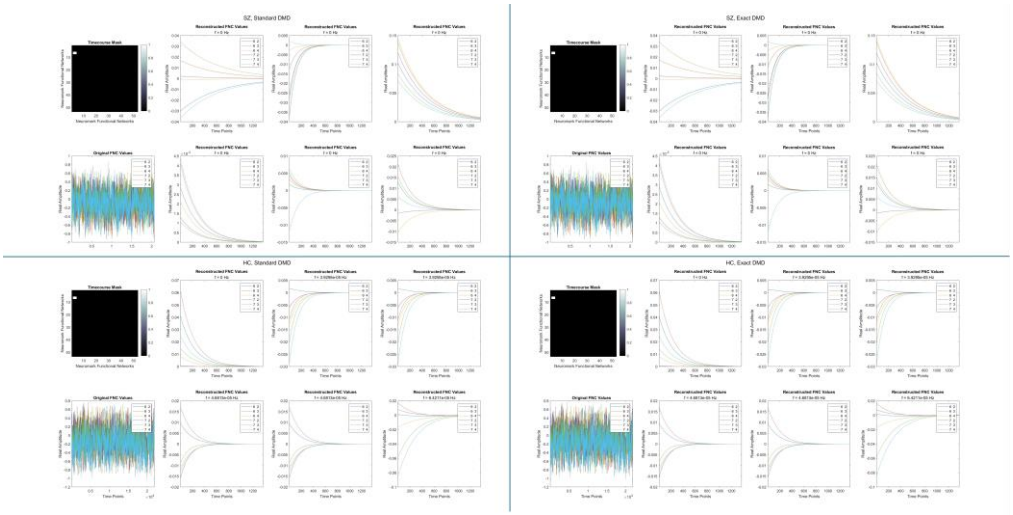

Removal of subject sFNCs changes group power spectra, and thus changes which modes are selected for time-resolved amplitude analysis. However, this does not qualitatively change results. Mode amplitudes continue to exponentially decay to zero over time, with no sign of oscillation. These decays are not universally monotonic: in schizophrenia, frequency 8.8701×10^{-5} Hz, one of the selected correlation coefficients rises in the first hundred time points before beginning its exponential decay, a feat repeated in one of the static control modes. Another control mode, frequency 8.8701×10^{-5} Hz, starts with negative amplitude and slightly overshoots zero before its decay begins. These are the exception, however, and no mode in either group maintains an amplitude far from zero beyond 785 samples.

sFNC Removed

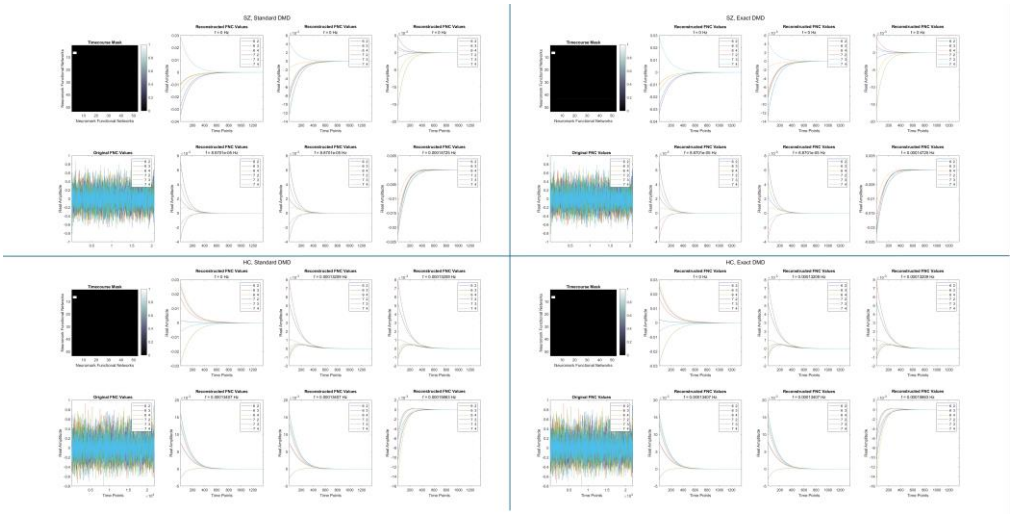

3.1.6. Spatial Structure of the Modes

As in the rest of this report, visible differences between standard and exact DMD are exceedingly minimal. Statistical tests should be run, but the author does not expect any significant differences to appear between methods. He proposes that all future analyses use exact DMD only.

Nonzero frequencies, such as $f = 1.6205 \times 10^{-4}$ Hz, have two or more associated spatial modes. These modes form conjugate pairs, i.e. their real parts are identical while their imaginary parts differ only in sign. Why these modes form conjugate pairs is not immediately clear to the author, although it is likely a feature of dynamic mode decomposition. Additional reading and study will be necessary to determine the cause of this phenomenon.

Visual comparison of the static patient modes and static control mode reveals no obvious similarities. Neither do visual comparisons of the dynamic modes reveal similarities, either in the spatial structure or, indeed, in their associated frequencies. Initial group-level decomposition suggests that patients and controls contain entirely different frequencies with negligible overlap between spatial maps. As these results are from only a single decomposition, it remains to be seen whether these results are stable.

Commented [DB1]: Need to code a test to confirm this.

sFNC Retained

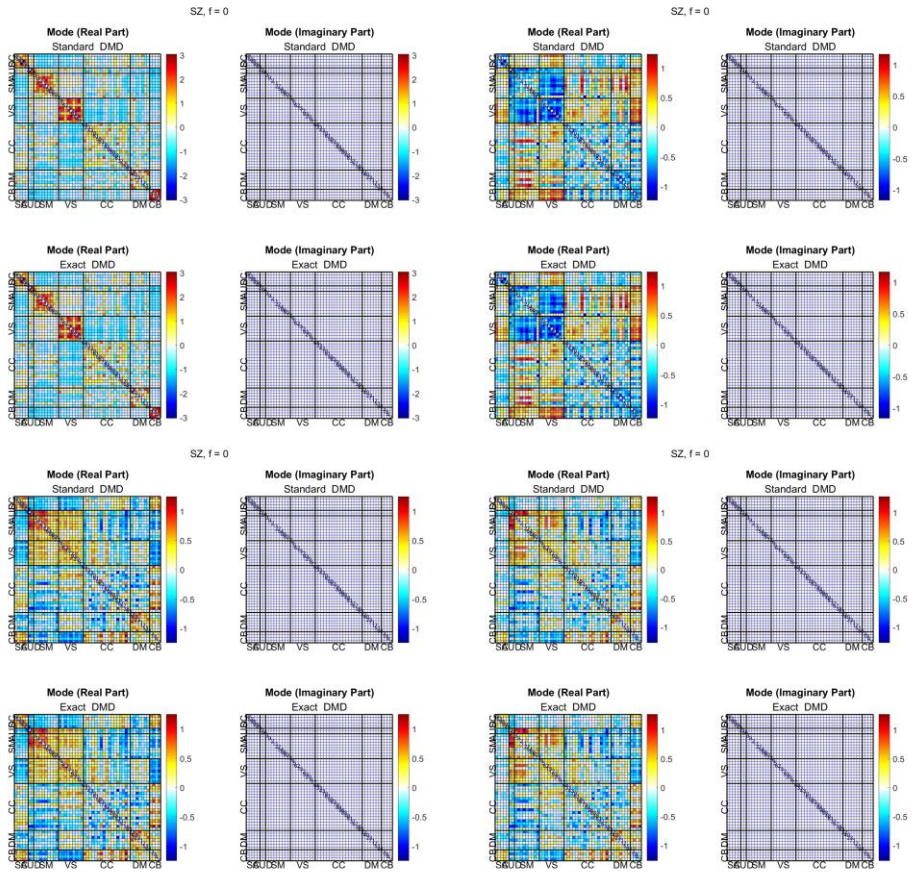
SZ, f = 0
Mode (Real Part)
Standard DMD
Mode (Imaginary Part)
Standard DMD
Mode (Real Part)
Standard DMD
Mode (Imaginary Part)
Standard DMD
Mode (Real Part)
Exact DMD
Mode (Imaginary Part)
Exact DMD
Mode (Real Part)
Exact DMD
Mode (Imaginary Part)
Exact DMD
SZ, f = 0
Mode (Real Part)
Standard DMD
Mode (Imaginary Part)
Standard DMD
Mode (Real Part)
Standard DMD
Mode (Imaginary Part)
Standard DMD
Mode (Real Part)
Exact DMD
Mode (Imaginary Part)
Exact DMD
Mode (Real Part)
Exact DMD
Mode (Imaginary Part)
Exact DMD
SMA UDSM VS CC DM CB

291

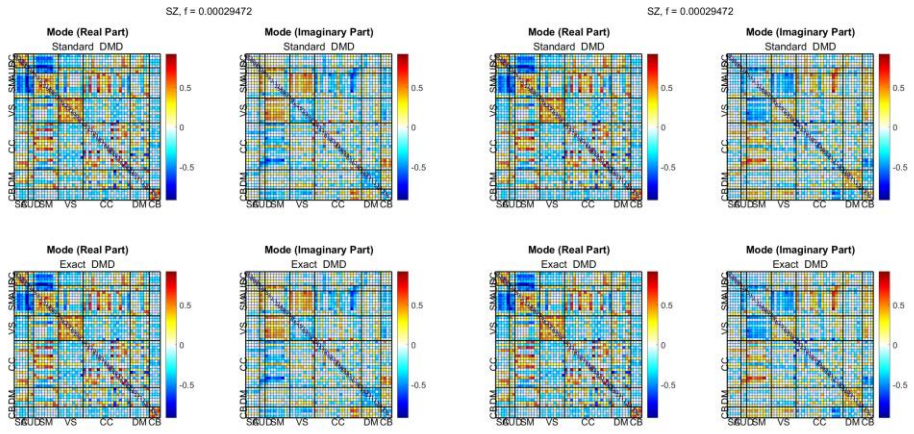
SZ, f = 0.00029472
Mode (Real Part)
Standard DMD
Mode (Imaginary Part)
Standard DMD
SZ, f = 0.00029472
Mode (Real Part)
Standard DMD
Mode (Imaginary Part)
Standard DMD
Mode (Real Part)
Exact DMD
Mode (Imaginary Part)
Exact DMD
Mode (Real Part)
Exact DMD
Mode (Imaginary Part)
Exact DMD
SM
UD
VS
CC
DM
CB

292

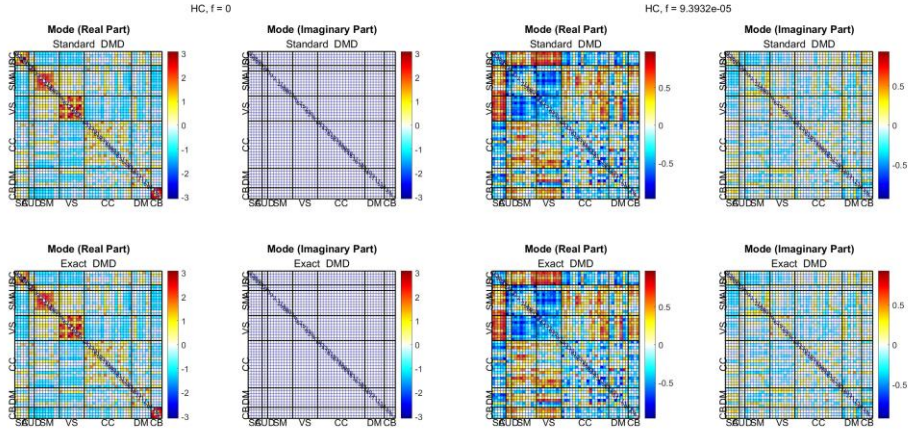
HC, f = 0
Mode (Real Part)
Standard DMD
Mode (Imaginary Part)
Standard DMD
HC, f = 9.3932e-05
Mode (Real Part)
Standard DMD
Mode (Imaginary Part)
Standard DMD
Mode (Real Part)
Exact DMD
Mode (Imaginary Part)
Exact DMD
Mode (Real Part)
Exact DMD
Mode (Imaginary Part)
Exact DMD
SM
UD
VS
CC
DM
CB

293

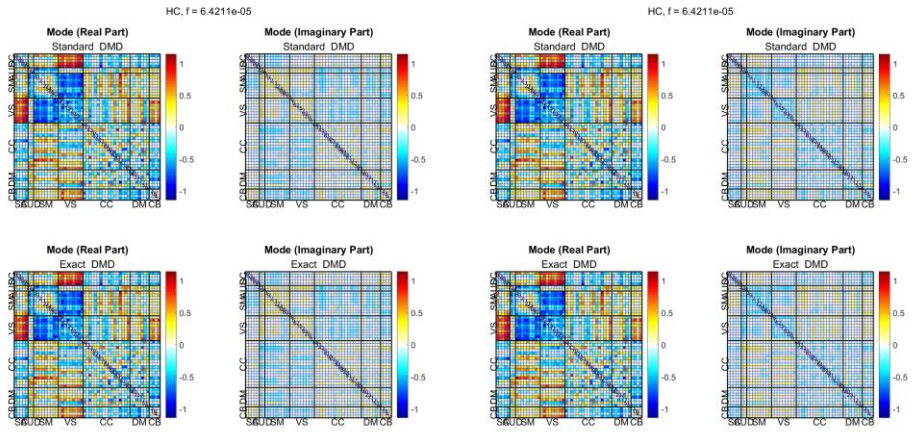

294
295

sFNC Removed 296

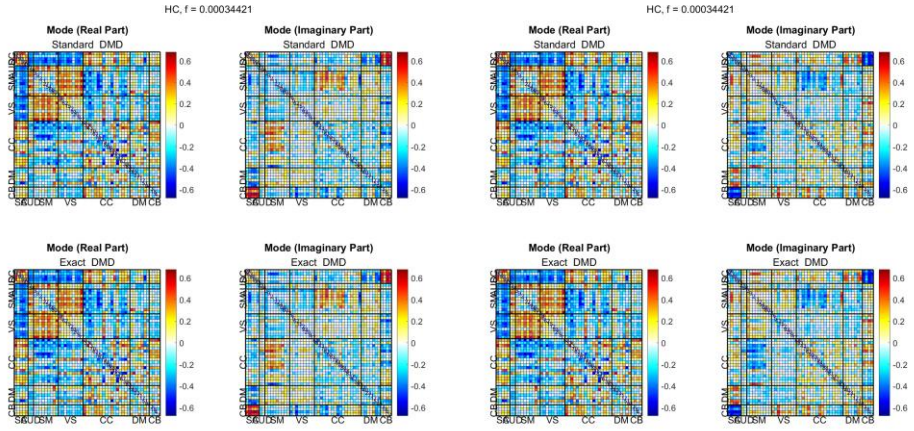

297

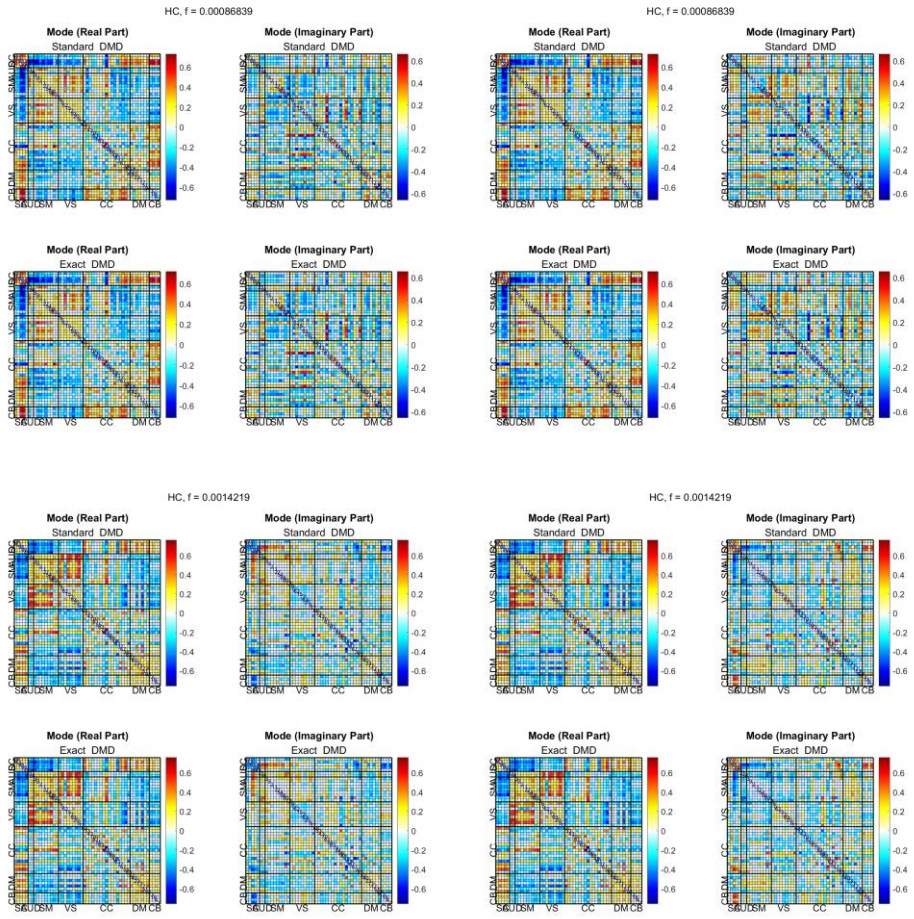
HC, f = 0.00086839
Mode (Real Part)
Standard DMD
Mode (Imaginary Part)
Standard DMD
HC, f = 0.00086839
Mode (Real Part)
Standard DMD
Mode (Imaginary Part)
Standard DMD
Mode (Real Part)
Exact DMD
Mode (Imaginary Part)
Exact DMD
Mode (Real Part)
Exact DMD
Mode (Imaginary Part)
Exact DMD
SM
VS
CC
DM
CB
0.6
0.4
0.2
0
-0.2
-0.4
-0.6

298

HC, f = 0.0014219
Mode (Real Part)
Standard DMD
Mode (Imaginary Part)
Standard DMD
HC, f = 0.0014219
Mode (Real Part)
Standard DMD
Mode (Imaginary Part)
Standard DMD
Mode (Real Part)
Exact DMD
Mode (Imaginary Part)
Exact DMD
Mode (Real Part)
Exact DMD
Mode (Imaginary Part)
Exact DMD
SM
VS
CC
DM
CB
0.6
0.4
0.2
0
-0.2
-0.4
-0.6

299

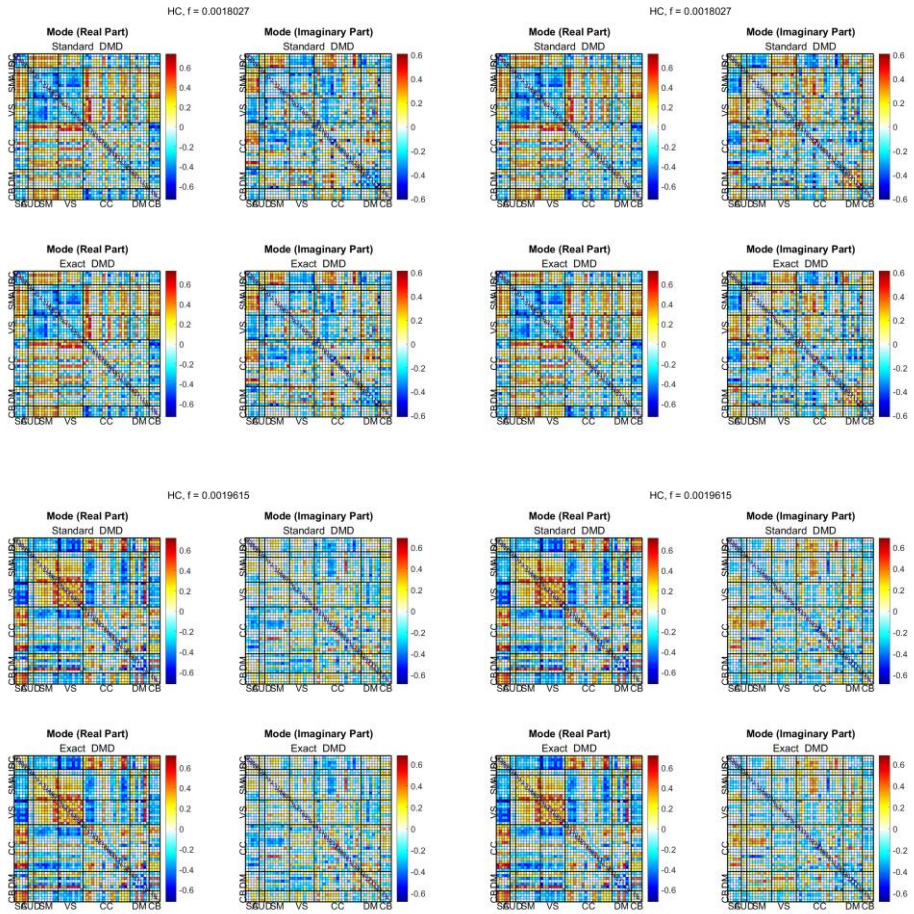
HC, f = 0.0018027
Mode (Real Part)
Standard DMD
Mode (Imaginary Part)
Standard DMD
HC, f = 0.0018027
Mode (Real Part)
Standard DMD
Mode (Imaginary Part)
Standard DMD
Mode (Real Part)
Exact DMD
Mode (Imaginary Part)
Exact DMD
Mode (Real Part)
Exact DMD
Mode (Imaginary Part)
Exact DMD
SM
UD
SM
VS
CC
DM
CB
0.6
0.4
0.2
0
-0.2
-0.4
-0.6

300

HC, f = 0.0019615
Mode (Real Part)
Standard DMD
Mode (Imaginary Part)
Standard DMD
HC, f = 0.0019615
Mode (Real Part)
Standard DMD
Mode (Imaginary Part)
Standard DMD
Mode (Real Part)
Exact DMD
Mode (Imaginary Part)
Exact DMD
Mode (Real Part)
Exact DMD
Mode (Imaginary Part)
Exact DMD
SM
UD
SM
VS
CC
DM
CB
0.6
0.4
0.2
0
-0.2
-0.4
-0.6

301

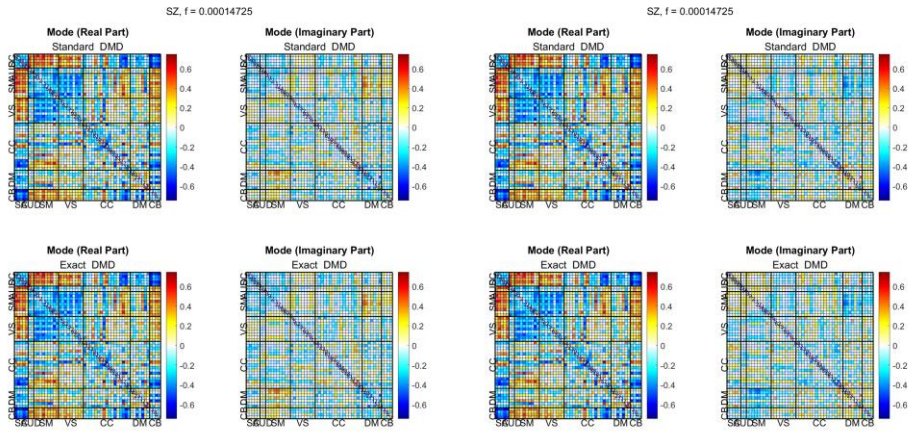
SZ, f = 0.00014725
Mode (Real Part)
Standard DMD
Mode (Imaginary Part)
Standard DMD
SZ, f = 0.00014725
Mode (Real Part)
Standard DMD
Mode (Imaginary Part)
Standard DMD
Mode (Real Part)
Exact DMD
Mode (Imaginary Part)
Exact DMD
Mode (Real Part)
Exact DMD
Mode (Imaginary Part)
Exact DMD
SMI UDSM VS CC DM CB
0.6 0.4 0.2 0 -0.2 -0.4 -0.6

302

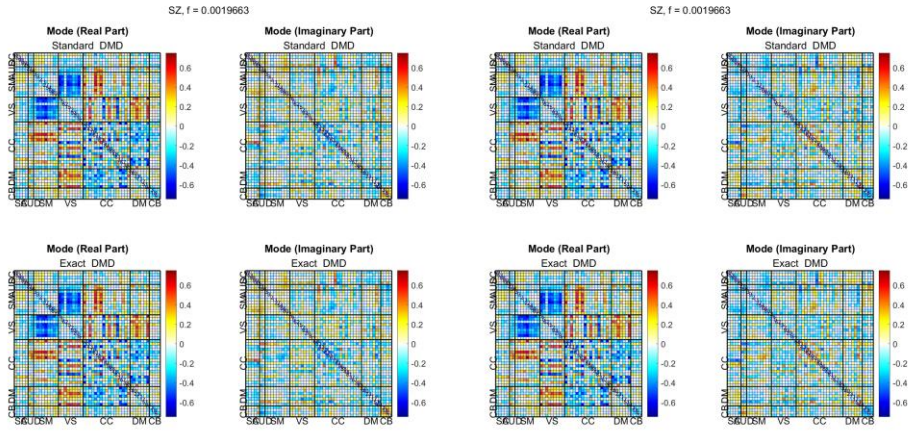
SZ, f = 0.0019663
Mode (Real Part)
Standard DMD
Mode (Imaginary Part)
Standard DMD
SZ, f = 0.0019663
Mode (Real Part)
Standard DMD
Mode (Imaginary Part)
Standard DMD
Mode (Real Part)
Exact DMD
Mode (Imaginary Part)
Exact DMD
Mode (Real Part)
Exact DMD
Mode (Imaginary Part)
Exact DMD
SMI UDSM VS CC DM CB
0.6 0.4 0.2 0 -0.2 -0.4 -0.6

303

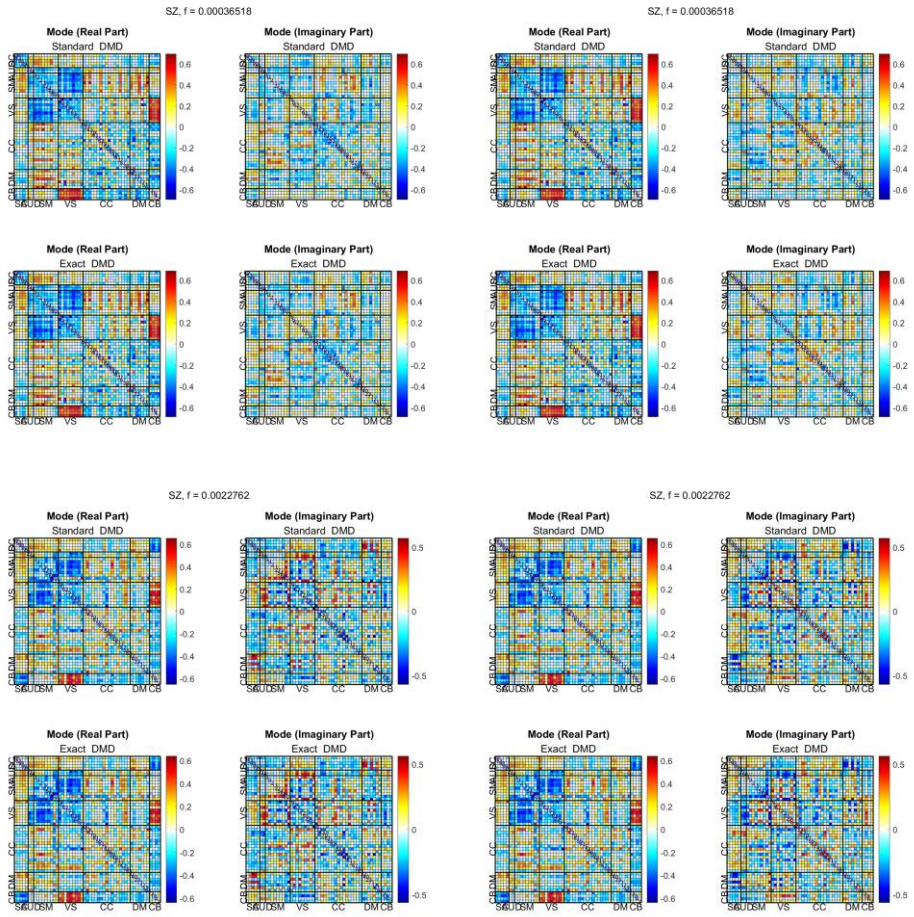
SZ, f = 0.00036518
Mode (Real Part)
Standard DMD
Mode (Imaginary Part)
Standard DMD
SZ, f = 0.00036518
Mode (Real Part)
Standard DMD
Mode (Imaginary Part)
Standard DMD
Mode (Real Part)
Exact DMD
Mode (Imaginary Part)
Exact DMD
Mode (Real Part)
Exact DMD
Mode (Imaginary Part)
Exact DMD
SZ, f = 0.0022762
Mode (Real Part)
Standard DMD
Mode (Imaginary Part)
Standard DMD
SZ, f = 0.0022762
Mode (Real Part)
Standard DMD
Mode (Imaginary Part)
Standard DMD
Mode (Real Part)
Exact DMD
Mode (Imaginary Part)
Exact DMD
Mode (Real Part)
Exact DMD
Mode (Imaginary Part)
Exact DMD
SM
UD
SM
VS
CC
DM
CB

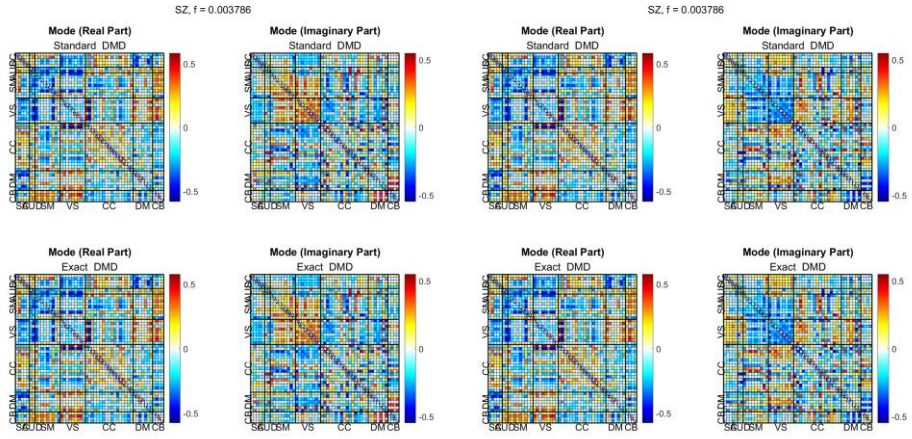
SZ, f = 0.003786
SZ, f = 0.003786
Mode (Real Part)
Standard DMD
Mode (Imaginary Part)
Standard DMD
Mode (Real Part)
Standard DMD
Mode (Imaginary Part)
Standard DMD
Mode (Real Part)
Exact DMD
Mode (Imaginary Part)
Exact DMD
Mode (Real Part)
Exact DMD
Mode (Imaginary Part)
Exact DMD
SM UD SM VS CC DM CB
0.5
0
-0.5

306
307

4. Next Steps

4.1. Corrections to Group Analysis

As described in the preceding report, several important questions on evaluating DMD analysis of dFNC remain to be answered. Mean squared error has proven deeply unreliable for estimating both the time-averaged and time-resolved accuracy of DMD-based signal reconstruction. An alternative means of estimating signal reconstruction must be identified. In addition, a suitable measure of "ground truth" for estimating the time-resolved goodness of signal reconstruction has not been identified, as the group average of a demeaned dFNC signal is necessarily near zero for all time points. Clearly, new methods for evaluating signal reconstruction must be discovered.

Group comparisons have, to date, exclusively been visual. This obviously does not meet scientific standards. Hypothesis tests must be implemented to determine whether group metrics differ significantly. These may first be applied to FNC matrices, in order to determine whether subject FNCs display notably altered structure between groups. Tests should also be run to confirm that exact and standard DMD produces statistically identical results.

Some rigorous means of comparing DMD mode spectra will be necessary. Nonparametric tests, such as the Kolmogorov-Smirnov test, may suffice to determine statistical alterations between groups, e.g. whether patients truly display reductions in mode power. It is likely possible to fit distribution functions to both unfiltered and demeaned spectra, which may allow for a parametric comparison between groups or subjects. This may, for instance, determine whether schizophrenia patients do indeed concentrate substantially more power in zero- or low-frequency modes, as visual inspection appears to suggest. However, detailed dissection of these spectra will require more advanced methods, likely pulled from signal analysis and information theory.

A more rigorous analysis of mode eigenvalues may help to predict their effect on system dynamics or detect meaningful differences between groups or subjects. Methods will likely need to be pulled from linear algebra. The author may need additional training in these fields to discover or develop such methods.

Comparing modes may be the most challenging step. Even a cursory glance at group power spectra reveals that, while distribution shape is similar, there are virtually no perfect frequency matches between groups. This renders frequency-based mode comparison unfeasible. Some alternative means of comparing modes between subjects and groups must be discovered. It may, for instance, be useful to compare modes via a distance matrix, with the goal of identifying modes with high spatial similarity between groups. This data could be interrogated in order to determine frequency's role in mode spatial similarities.

Comparison of modes is not merely a spatial problem, but a temporal one as well. Modes vary in amplitude over time, and so their trajectories and dynamic parameters require comparison as well as their spatial structure. An obvious starting position is to fit reconstructed mode dynamics using estimated eigenvalues as a fixed parameter. While such a fit may be easily accomplished using eigenvalue magnitudes, this omits phase information and is in any case a far from complete parameterization of mode dynamics. Additional information must be drawn from the available data, likely from differential equation and dynamic system theory. The author may need additional training in these fields to discover or develop such methods.

4.2. Subject Visualizations

Before subject-level analysis commences, it will be necessary to visualize several sample subjects to determine what questions may be sensibly asked. The author will adapt the current group-level visualizations to this end. Two subjects' demeaned data will be visualized, one from each group. Visual results should parallel those presented in this report.

4.3. Group Distributions

Subject-level analyses will produce subject-level modes and spectra. Some means of analyzing the distributions of these modes and spectra will likely prove very useful. However, as both spectra and modes are high-dimensional variables (136 and 1378 dimensions, respectively), the multiple-comparison problem and central limit theorems may complicate the comparison of their distributions.

Comparing mode distributions may be feasible via the network-based statistic [2], [3], [4] or simple application of a multiple comparison correction to group-level differences in connectivity maps. The author recalls that several members of the group, most notably Amritha and KuaiKuai, have conducted such analyses in the past.

4.4. Independent Mode Decomposition

4.5. Comparable Mode Decomposition

4.6. Clinical Scores

It may be worth comparing subject-level spectra to clinical or behavioral scores to determine whether any frequencies show links to behavioral effects. If so, an examination of the affected modes could provide useful insights into connectivity biomarkers for such behaviors. This analysis may need to account for interaction effects.